EUROPEAN ENDODONTIC JOURNAL

ORIGINAL ARTICLE

Cyclic Fatigue, Torsional Strength and Angular Deflection of Different Reciprocating Instruments: A Critical Analysis of Its Clinical Relevance

Javier CAVIEDES-BUCHELI,[1] Abel TEVES-CORDOVA,[2] Murilo Priori ALCALDE,[3] Hugo Roberto MUNOZ,[4] Hernan Dario MUÑOZ-ALVEAR,[5] Monique Marie GAY,[6] Ricardo PORTIGLIATTI,[7] Jose Francisco GOMEZ-SOSA,[8,9] Jorge OLMOS-FASSI,[10] Marco Antonio Hungaro DUARTE[3]

[1]Dentistry Research Center, Pontifical Javeriana University, School of Dentistry, Bogotá, Colombia
[2]Bauru School of Dentistry, São Paulo, Brazil
[3]Department of Dentistry, Endodontics and Dental Materials, Bauru School of Dentistry, São Paulo, Brazil
[4]Department of Endodontics, University of San Carlos de Guatemala, Guatemala City, Guatemala
[5]Postgraduate Endodontics Department, Cooperative University of Colombia, School of Dentistry, Pasto, Colombia
[6]Department of Endodontics, University of Santo Tomas, School of Dentistry, Bucaramanga, Colombia
[7]Postgraduate Program of Endodontic Specialization Training, University of Buenos Aires, Buenos Aires City, Argentina
[8]Cell Therapy Unit, Venezuelan Institute of Scientific Research, Caracas, Venezuela
[9]Department of Endodontics, University of Santa Maria, School of Dentistry, Caracas, Venezuela
[10]National University of Tucumán, School of Dentistry, Tucumán, Argentina

ABSTRACT

Objective: To evaluate the cyclic fatigue fracture resistance, torsional fatigue, and angular deflection of Reciproc Blue (RB), WaveOne Gold (WOG), One Reci (OR), and Plex RC-One (RC-One) instruments for managing root curvatures in simulated canals.

Methods: A sample size calculation determined 10 samples per group (5 instruments for the cyclic fatigue test and 5 for the torsional fatigue test) for detecting significant differences. The study included 40 NiTi instruments (25 mm) from four reciprocating systems groups: RB R25, WOG 25, OR 25, and RC-One 25. Instruments were inspected for defects. Bending tests assessed memory control. Static cyclic fatigue tests used an artificial 60° curved canal with motorized activation. Torsional fatigue followed ISO 3630-1, measuring torque and angular deflection until failure. Fractured surfaces were analyzed using automated image analysis and measured with Rhinoceros 8.0 software. Statistical analysis included central tendency and dispersion measures, followed by ANOVA to identify statistically significant differences between groups.

Results: The bending test showed RC-One retained shape after pressure, while RB exhibited moderate resistance. WOG and OR did not demonstrate satisfactory bending resistance. Analysis of cyclic fatigue revealed RC-One had the highest resistance, followed by RB, OR, and WOG ($p<0.001$). RB required the highest torque for fracture, followed by RC-One, WOG, and OR ($p<0.001$). WOG had the lowest deflection angle at fracture, followed by OR, RB, and RC-One ($p=0.0399$). SEM and intelligent automated image processing analysis showed RC-One and RB had wear zones indicative of slow fracture, while WOG and OR displayed 100% rapid fracture dimples. RC-One had 41.86% slow fracture and 54.14% rapid fracture, while RB had 17.83% slow and 82.17% rapid fracture. Torsion tests revealed similar features in RC-One and RB, supporting their high and similar torsional resistance and deflection, unlike WOG's lower resistance and OR's lowest resistance with the highest deflection.

Conclusion: The best performance in the bending test was obtained by RC-One, followed by RB, while most failures were observed in WOG and OR. RC-One showed significantly higher cyclic fatigue resistance in severe curvatures than RB, WOG, and OR. RB and RC-One exhibited very similar torsional resistance values, significantly higher than OR and WOG. RC-One displayed superior angular deflection results compared to the other instruments.

Keywords: Angular deflection, cyclic fatigue resistance, NiTi instruments, root canal curvatures, torsional fatigue

Please cite this article as: Caviedes-Bucheli J, Teves-Cordova A, Alcalde MP, Munoz HR, Muñoz-Alvear HD, Gay MM, et al. Cyclic Fatigue, Torsional Strength and Angular Deflection of Different Reciprocating Instruments: A Critical Analysis of Its Clinical Relevance. Eur Endod J 2025; 10: 159-172

Address for correspondence: Javier Caviedes-Bucheli
Dentistry Research Center, Pontifical Javeriana University, School of Dentistry, Bogotá, Colombia
E-mail: javiercaviedes@gmail.com

Received : August 24, 2024,
Revised : October 07, 2024,
Accepted : October 25, 2024

Published online: March 18, 2025
DOI 10.14744/eej.2024.08860

HIGHLIGHTS

- The clinical applicability of the results obtained in cyclic fatigue, torsional fatigue, angular deflection, and bending tests in the management of curved canals.
- The concept of slow fracture and rapid fracture and its clinical applicability in the use of reciprocating instruments as a preventive control mechanism for instrument fractures by deforming before failure.
- The bending test is a mechanism to evaluate the controlled memory of instruments, which is crucial for preserving the original anatomy of the canal and for resistance to cyclic and torsional stress by adapting to and respecting the canal's original shape.
- The influence of conducting the study at body temperature and its direct clinical analogy in the behavior of alloys regarding cyclic and torsional fatigue resistance, as well as in the bending test.
- The advancement of intelligent automated image processing, specifically in image recognition, to determine areas of rapid and slow fracture to quantify these zones.

INTRODUCTION

Instrument fractures in endodontics at a clinical level are considered a situation of maximum stress for the professional (1). The incidence of fracture of nickel-titanium (NiTi) instruments ranges between 1.3%–10.0% (2), where it has been reported that 93.6% of endodontists have experienced instrument fractures in the clinical practice of their profession. Instruments fractures generates additional time for the clinician to extract it and puts the success of the treatment at risk (3).

Two fracture mechanisms of endodontic instruments have been described: cyclical flexural and torsional fatigue. Flexural cyclic fatigue is characterized by the tension/compression cycles that the instrument experiences at the point of its maximum flexion in a curvature (4, 5). This mode of failure is attributed to the repetitive stresses exerted on the outermost fibers of the file while rotating in a curved root canal, leading to eventual fracture. On the other hand, torsional fatigue occurs when the tip of an instrument binds to the canal wall, causing the stem to continue rotating and surpassing the elastic limit of the metal, resulting in instrument fracture (6).

Additionally, the angular deflection must be considered. This property represents the deformation a file can withstand before a torsional failure when the file is rotating. This property is evaluated in degrees, and a higher deflection angle indicates that the file can undergo both plastic and elastic deformation when the tip is blocked, thus avoiding fracture of the instrument (4, 5).

The skill of the operator influences these two types of fractures and angular deflection, his knowledge of the anatomy knowledge in the preparation of curved root canals, and kinematics of the instruments (7).

The design and manufacturing of the instruments are also factors of great importance. The tip, the transition angle, cutting angles, edges, and helical angle of the instrument also influence its resistance to fracture (7, 8). On the other hand, kinematics will also influence this resistance, where reciprocating movement has been shown to improve endurance compared to continuous rotational movement (8).

The instrument alloy is subjected during its manufacturing to heat treatment processes that change its metallographic expression according to the austenite-martensite transformation phases, both at room temperature and at 37°C, which also modifies its resistance to different causes of fracture (8).

This treatment involves continuous heating and cooling, which alters the properties of the alloy and induces oxidation of the surface layer, resulting in distinctive colors such as gold, blue or cobalt (9). These changes significantly improved the instruments' resistance to cyclic fatigue, both in terms of flexural and torsional stresses, and enhanced their flexibility compared to conventional superelastic wires (10).

Alloys with controlled memory (CM) have also been developed, characterized by being in the martensitic phase at body temperature. Owing to their exceptional flexibility and memory control, these wires are particularly well-suited for navigating complex anatomies, including severe curvatures, while enhancing resistance to flexural fatigue (11).

With these types of advances in instrument design and alloy evolution, the analysis of cyclic flexural and torsional fatigue studies does not report a correlation with clinical practice, as it takes a purely technical approach. However, its results cannot be separated from the clinical application (12).

Therefore, it is important to carefully analyze the selection of an instrument for managing a given root canal curvature. The influence of the instrument's design, the alloy composition, and the type of movement employed all contribute to generating greater security and efficacy in managing varying degrees of canal curvature (13).

For this reason, this study compared four reciprocating instruments with similar characteristics in their design and types of latest generation alloys including Reciproc Blue (RB), WaveOne gold (WOG), One Reci (OR), and Plex RC-One (RC-One), to provide a clinical response to cyclic fatigue studies, which can be achieved through a clear and repeatable methodology with study models that closely approximate clinical reality (12).

Instrument fractures often combine cyclic and torsional fatigue (14), These tests should be performed at body temperature (37°C) to resemble a patient's clinical conditions, and it could be inferred which instrument is the safest in managing

severe curvatures, having the lowest probability of fracture, and preserving the original anatomy of the canal as much as possible during endodontic therapy (15).

Therefore, the purpose of this study is to evaluate the cyclic fatigue fracture resistance, torsional fatigue, and angular deflection levels of the RB, WOG, OR, and RC-One instruments, and to determine which instrument is the safest in the management of root curvatures in simulated canals.

MATERIALS AND METHODS

This study was conducted in accordance with the Declaration of Helsinki and approved by the ethics committee of Santa Maria University under the number CBUSM-0723 dated 03/15/2023 and following the PRILE guidelines (Fig. 1). The sample calculation was performed based on previous study using G*Power v3.1 for Mac (Heinrich Heine, University of Düsseldorf, Düsseldorf, Germany) by selecting the ANOVA: Fixed effects, omnibus, one-way of the F test family (16–22) (Table 1). An alpha-type error of 0.05, a beta power of 0.95, and an effect size of 0.80 were used. The six initial results of each test were taken into consideration. For the time to fracture, maximum torque, angle of rotation, and maximum load tests, a total of 8 instruments per group were determined, respectively. Then, a final sample size was set at 10 instruments per group for each test.

In this study, a total of 40 (n=10 per instrument studied) NiTi instruments (length=25 mm) from four different reciprocating systems with a tip diameter of 25 were included: RB R25 (size #25, taper 0.08 taper 5% from mm^3), WOG 25 (size #25, 0.07 taper 5% taper, from mm^3), OR 25 (size #25, 0.06 taper), and RC-One 25 (size #25, 0.06 taper). Table 1 presents the characteristics of the studied instruments. Before testing, all instruments underwent a thorough inspection for structural defects using a stereomicroscope (Carl Zeiss, LLC, Oberkochen, Germany) at 16x magnification, with none being excluded from the study. Each instrument used in the study was standardized at a length of 25 mm, with 10 instruments from each brand allocated for cyclic and torsional fatigue testing.

Bending Test

A bending test was conducted to assess the memory control capacity of the file. The file handle was securely fixed in a vise, and a calibrated force of 2.5 newtons was applied to the tip using a dynamometer. The stem was then rotated counterclockwise while attempting to maintain the file at an angle of at least 45°, preventing longitudinal movement. This test evaluated the file's ability to retain its curved shape or straighten under the applied force.

Static Cyclic (Flexural) Fatigue Test

This test was conducted using a stainless-steel device equipped with an artificial canal to accommodate five 25 mm instruments from each system, with a 0.2 mm margin to facilitate movement; the size and taper of each instrument were replicated by inserting a guide cylinder, enabling a consistent simulation of an instrument confined within an artificial curved canal with a 60° curvature angle, 5 mm radius, and the center of curvature positioned 5 mm from the tip, as outlined in previous studies (22) (Fig. 2a, b); the arch and guide cylinder included a 1 mm deep slot 5 mm from the top to match the contra-angle height, allowing the instrument to remain curved and freely rotate between the cylinder and external arc; each reciprocating system's five instruments were activated using a 6:1 reduction handpiece driven by a motor with controlled torque (Silver Reciproc, VDW), with all rotary motion systems operated at 150/30 turning angles and 300 rpm to ensure standardized conditions, while a high-flow synthetic oil (Super Oil; Singer Co Ltd, Elizabethport, New Jersey) was applied to minimize friction; timing began upon motor activation and ceased immediately upon visual and/or audible detection of instrument fracture, recorded using a digital timer, with video recording conducted simultaneously to capture the exact moment of fracture for further analysis.

Torsional Fatigue Test

Torsional fatigue tests were conducted following the guidelines outlined in ISO 3630–1 (2019E) using a torsion machine as previously described (23). This testing aimed to determine the average torque values and the maximum angular deflection necessary for each instrument until failure.

Torque values were assessed by measuring the force exerted on a small load cell through a lever arm linked to the torque axis. The rotation angle was monitored and controlled using a resistive angular transducer connected to a process controller. Before testing, the handle of each instrument was removed at the point where it was attached to the shaft. The end of the shaft was secured to a chuck connected to a reversible gear motor. The instrument's tip, 3 mm from its end, was clamped in another chuck with brass jaws to prevent slippage (Fig. 3a). The counterclockwise rotation speed was set to 2 rpm. The maximum resistance to torsion and angular rotation was recorded, which were reported in newtons and degrees using a specifically designed computer program (Analógica, Belo Horizonte, MG, Brazil) (Fig. 3b). All tests were conducted at 37°C body temperature to simulate the clinical conditions of a patient (24).

Descriptive Area Analysis

A descriptive analysis of the fractured surfaces of the instruments was conducted by selecting a random sample from each file. Photomicrographs were captured and imported into an image software as follows: Image processing was performed using ImageJ by converting the image to grayscale to increase contrast and highlight the edges and dimples. Subsequently, the image was binarized to separate the dimples from the background, adjusting the necessary threshold. The edges were then segmented to determine the contours of the dimples, allowing the marking of the rapid and slow fracture zones. Finally, zonal division was performed, calculating the size and density of the dimples to classify them into slow and rapid fracture zones. Then images were imported into the Rhinoceros 8.0 software, which allows for the reconstruction of curves and surfaces that can be mathematically evaluated. This software enabled the measurement of areas, volumes, and perimeters in the images with a margin of error of less than 1% (24, 25). Through this process, the areas of rapid and slow fracture were observed, allowing for an analysis of cyclic fatigue and an explanation of the results obtained in the study. The images were imported into the software, and the measurement scales in microns were programmed. The scaling was then carried out us-

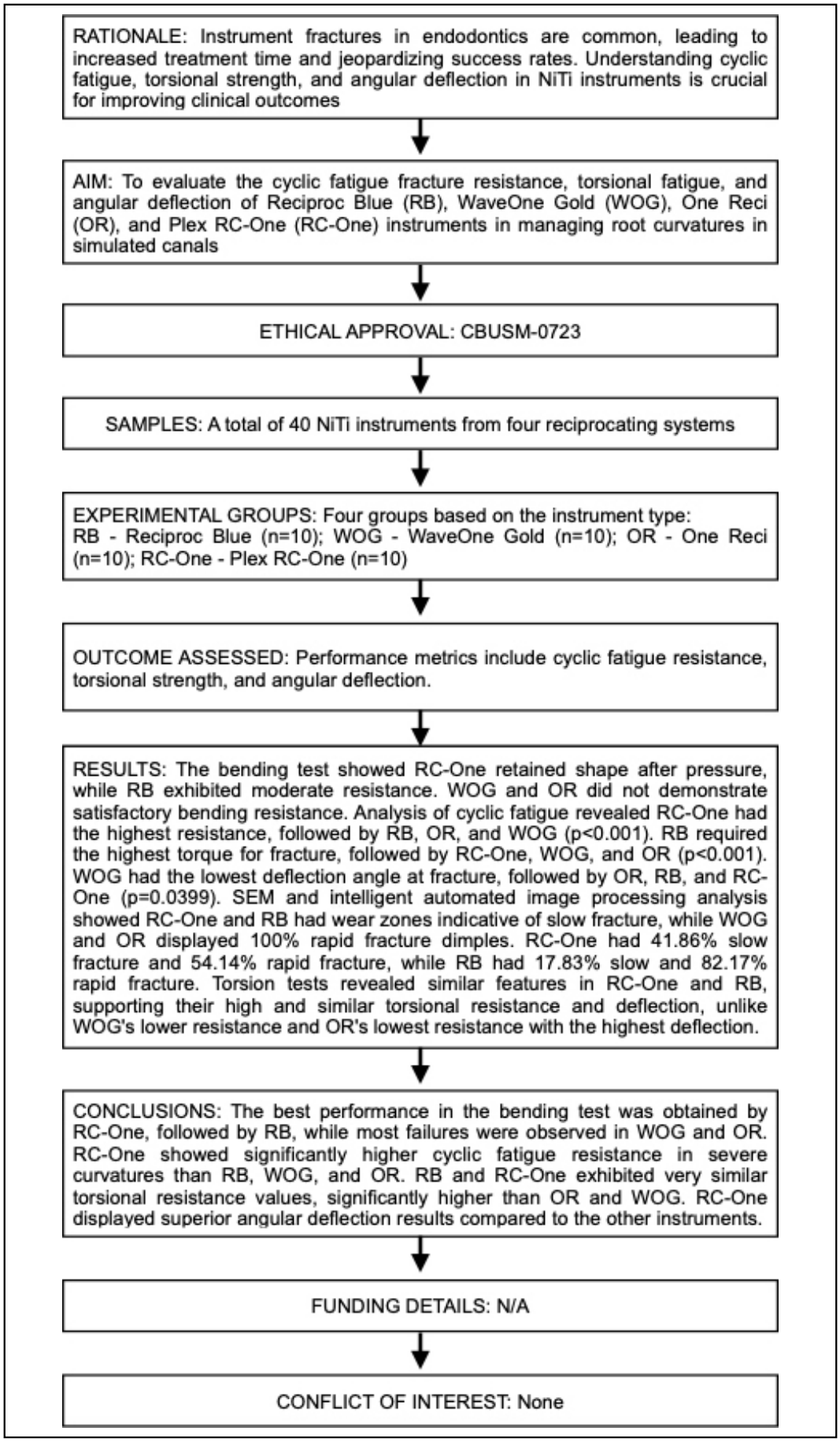

Figure 1. PRILE flowchart

TABLE 1. Characteristics of the studied reciprocating files

Reciprocating system	Motion	Speed	Tip	Transition angle	Taper	Helical angle	Section profile	Alloy
Reciproc blue (16, 17)	150/30	300 rpm	Inactive	Large	Variable 8% first 3 mm. 4% of 3–6 mm and 5% of 6–16 mm	Variable	S Shape	Martensitic Blue heating 550°C Cooling 120°C
Wave One Gold (WOG) (18)	150/30	350 rpm	Semi active	Large	Variable 7% first 3 mm. 6% of 4–10mm 3% of 10–16 mm	Constant	Rectangular shape	Martensitic Gold heating 400°C Cooling 120° C
OneReci (OR) (19, 20)	170/60	350 rpm	Inactive	Short	6% constant	Variable	Triangular Variable triple helix up to 4mm 4–6mm transition zone S shape 6–16mm	Martensitic Cobalt heating 700°C Cooling 120°C electropolished finish
Plex RC - One (RC-One) (21)	160/40	500 rpm	Inactive	Short	6% Constant	Variable	Modified convex triangular in the first three mm S shape 6-16 mm	Martensitic Silver Modify at 37°C electropolished finish

RC: Reciproc Blue

TABLE 2. Resistance to cyclic fatigue in seconds of 4 types of files

File	N	Mean	SD	Min	Max
Reciproc Blue	5	282.4	45.51	240	360
WaveOne Gold	5	124.2	27.11	83	146
OneReci	5	221.2	25.67	180	248
Plex RC-One	5	1215.8	282.47	730	1735

Anova p<0.0001. Tukey's post hoc test showed statistically significant differences between Plex RC-One and the three other instruments (Reciproc Blue p=0.001, WaveOne Gold p=0.001, OneReci p=0.001). SD: Standard deviation, Min: Minimum, Max: Maximum

TABLE 3. Torque in Newtons of 4 types of files at the time of fracture

File	N	Mean	SD	Min	Max
Reciproc Blue	5	1.72	0.15	1.5	1.9
WaveOne Gold	5	1.16	0.05	1.1	1.2
OneReci	5	0.44	0.09	0.3	0.5
Plex RC-One	5	1.32	0.19	1.0	1.6

Anova p<0.0001. Tukey's post hoc test showed statistically significant differences between all pairwise comparisons, except for Plex RC-One and Reciproc Blue p=0.1034

ing the guides present in the photomicrographs, and the cyclic fatigue zones were drawn on the image using the curve with the control points command. Finally, the analyze command was used to obtain the physical properties and area, taking the total silhouette of the fractured surface of the file as 100%. This was followed by the evaluation of the slow and rapid fracture zones, with the measurements recorded in an Excel database to calculate the percentage of the analyzed areas.

Statistical Analysis

Statistical analysis was conducted for each of the files analyzed, presenting measures of central tendency (mean) and dispersion (standard deviation, minimum, and maximum values) to describe the cyclic fatigue behavior in terms of the time until fracture in seconds, as well as torsion (N) and deflection angle in degrees. A Kolmogorov-Smirnov test was used to verify if the data presented a normal distribution. Subsequently, an ANOVA test was carried out to determine if there were statistically significant differences among the various files assessed. Finally, Tukey´s post hoc test was used for pairwise comparisons.

RESULTS

During the bending test, the RC-One file retained its shape after the applied pressure, while RB exhibited moderate resistance to bending. In contrast, WOG and OR did not demonstrate satisfactory levels of bending resistance (Fig. 4a, b).

The analysis of cyclic fatigue resistance, as detailed in Table 2, revealed a significant difference in the time until fracture, with RC-One demonstrating the highest resistance, followed by RB, OR, and WOG, respectively (Anova p<0.001).

Table 3 describes the behaviour of the torque in Newtons required for fracture, finding that it was significantly higher in the RB file, followed by RC-One, WOG, and finally OR (Anova p<0.001).

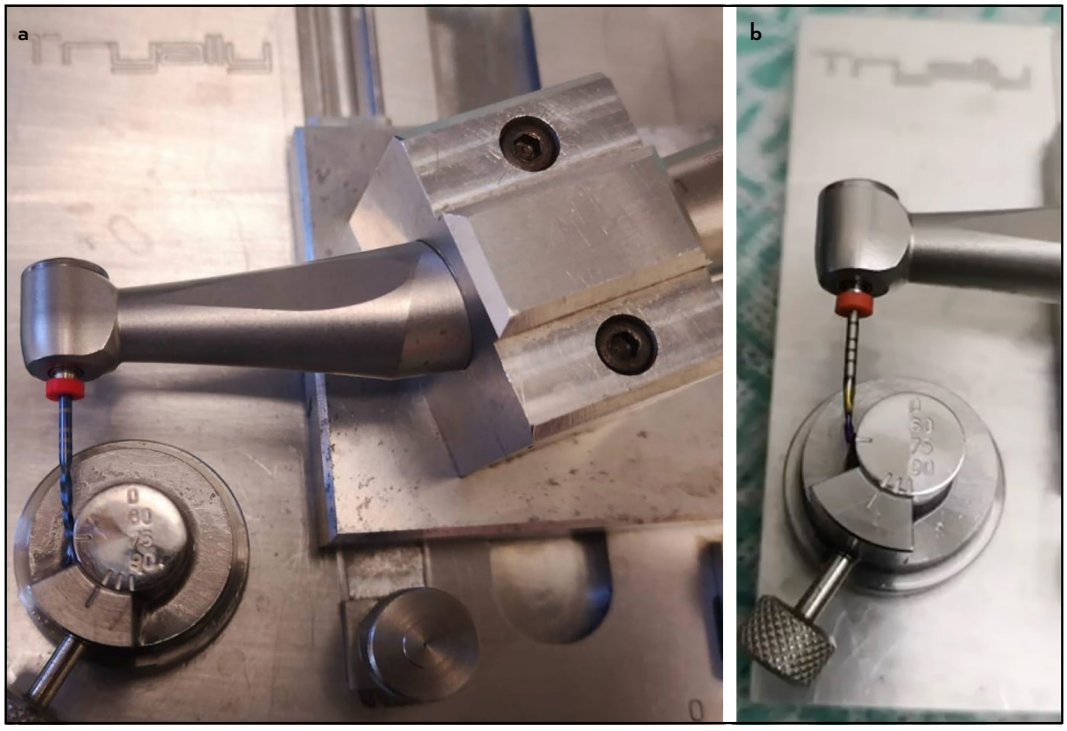

Figure 2. (a) Image of the system used for the cyclic fatigue test. (b) Close-up image of the system showing the 60-degree angle and 5mm radius forming parameters used for the cyclic fatigue test

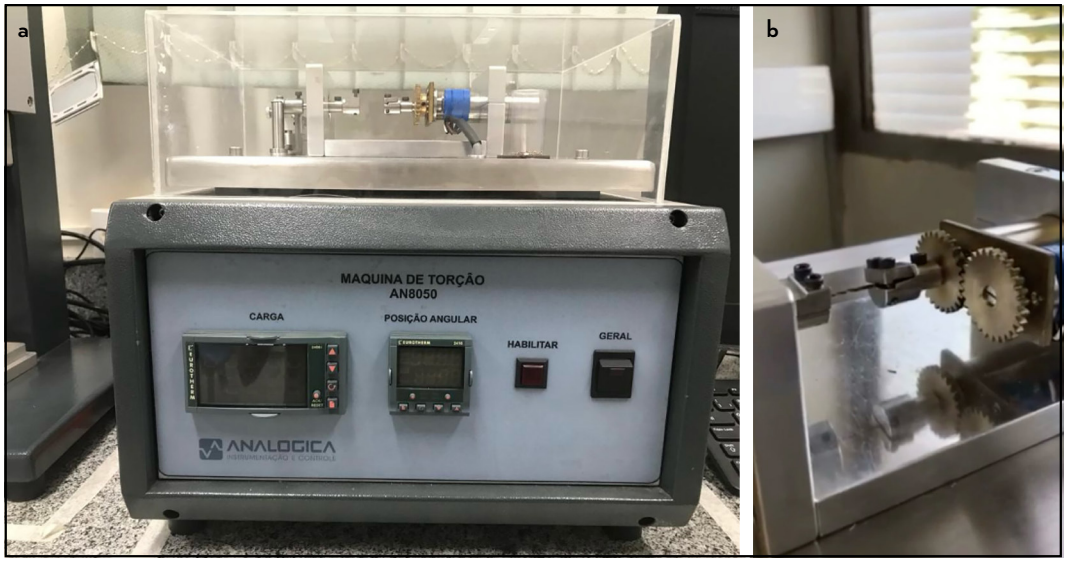

Figure 3. (a) Image of the universal testing machine used for torsional testing. (b) Closer image showing the instrument positioned for torsional testing

Table 4 outlines the behaviour of the deflection angle in degrees at the moment of fracture, revealing that it was significantly lower in the WOG file, followed by OR, RB, and finally RC-One (Anova p=0.0399).

SEM analysis of the fractured surfaces revealed the presence of cyclic fatigue zones characterized by rapid or ductile fracture, marked by large dimples and areas exhibiting wear or metal deformation before failure. At 100x magnification, distinct wear zones were observed in the RC-One and RB files (Fig. 5c, e), unlike the OR and WOG files, which displayed 100% dimple formations indicative of rapid fracture. At 1000x magnification, the RC-One showed a 41.86% slow fracture area and 54.14% rapid fracture area (Fig. 5h), while RB exhibited a 17.83% slow fracture area and 82.17% rapid fracture area (Fig. 5b). In contrast, WOG and OR files did not present any slow fracture areas, displaying 100% dimples characteristic of rapid fracture (Fig. 5d-f) (Table 5). The torsion test revealed concentric abrasion marks and fibrous dimple marks in the center of rotation for all instruments, indicating torsional failure. The RB and RC-One images (Fig. 6a-g) were very similar, with larger features observed in the WOG and OR (Fig. 6c-e), supporting the results where RC-One and RB exhibited high and similar torsional fracture values, accompanied by comparable angular deflec-

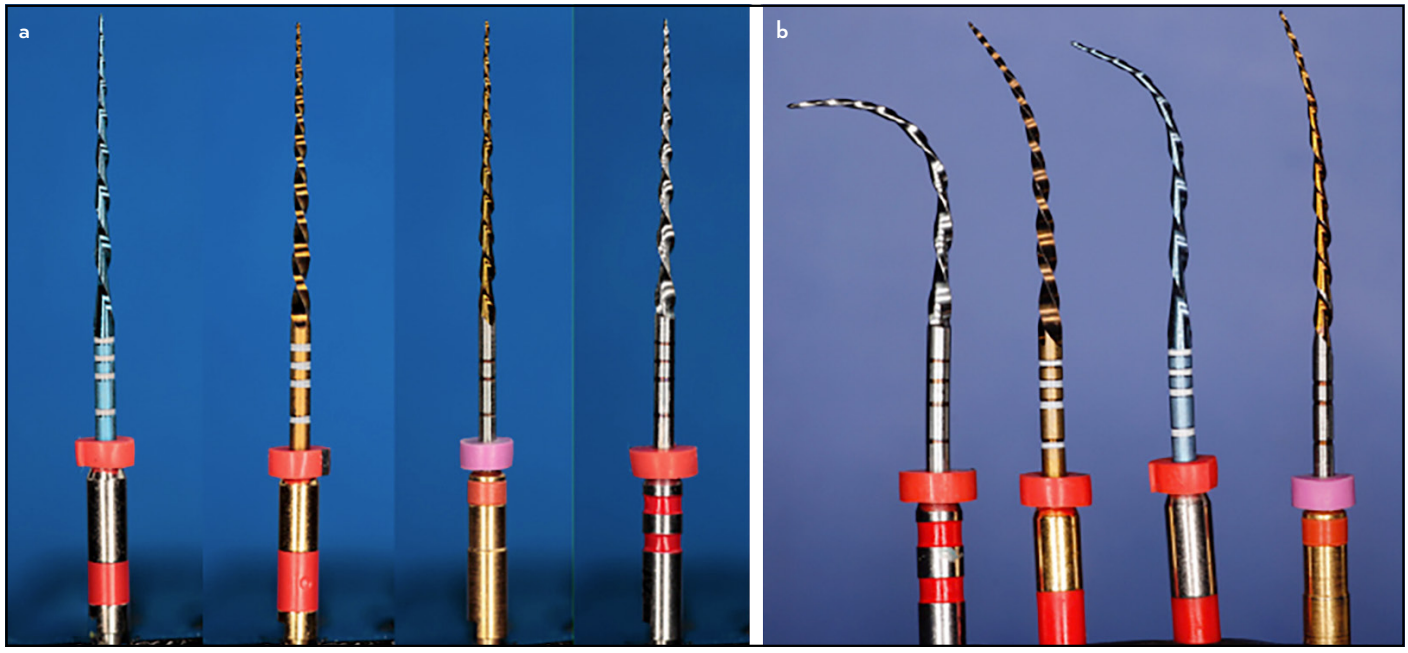

Figure 4. (a) The Reciproc Blue (RB), WaveOne Gold (WOG), One Reci (OR), and Plex RC-One (RC-One) files before the bending test. (b) Results of the flexural and controlled memory test, demonstrating each file's ability to maintain its curved shape or straighten under applied forces. The Plex RC-One file exhibited the greatest flexibility and controlled memory, followed by Reciproc Blue. In contrast, One Reci and WaveOne Gold displayed the least flexibility and controlled memory

TABLE 4. Deflection angle at the moment of fracture of 4 different types of files

FILE	N	Mean	SD	Min	Max
Reciproc Blue	5	399.54	39.25	365.7	464.2
WaveOne Gold	5	290.38	16.80	270.4	314.4
OneReci	5	390.69	91.42	202.9	484.7
Plex RC-One	5	414.30	65.65	329.1	504.7

Anova p=0.0399. Tukey's post hoc test showed statistically significant differences only between WaveOne Gold and Plex RC-One (p=0.03), and between WaveOne Gold and Reciproc Blue (p=0.045)

tion, unlike the WOG, which presented lower resistance to torque and less angular deflection, and the OR, which showed the lowest torsional resistance but highest angular deflection.

DISCUSSION

Cyclic fatigue studies often face criticism for their limited clinical applicability, primarily due to insufficient interpretation and correlation between study models and the characteristics of instruments used in practice. While *in vitro* studies control all variables to replicate clinical conditions, their findings must maintain clinical relevance to be valuable. When designed with scientific rigor, these studies can lay a solid foundation for future clinical research (26).

TABLE 5. SEM analysis of the fractured surfaces revealed the presence of cyclic fatigue zones

System	Cyclic fatigue					
	100x			1000x		
	Area	Area um²	Area %	Area	Area um²	Area %
RB	Area total	227269.35	100	Area total	11785.74	100
	Slow fracture area	70866.83	31.18	Slow fracture area	2101.91	17.83
	Rapid fracture area	298136.18	68.82	Rapid fracture area	9683.83	82.17
WOG	Area total	170329.48	100	Area total	11833.72	100
	Slow fracture area	0.00	0.00	Slow fracture area	0.00	0.00
	Rapid fracture area	170329.48	100.00	Rapid fracture area	0.00	0,00
OR	Area total	49086.87	100	Area total	11964.40	100
	Slow fracture area	0.00	0.00	Slow fracture area	0.00	0.00
	Rapid fracture area	49086.87	100.00	Rapid fracture area	0.00	0.00
RC-One	Area total	58053.12	100	Area total	12032.07	100
	Slow fracture area	24302.28	41.86	Slow fracture area	4964.25	41.26
	Rapid fracture area	33750.84	58.14	Rapid fracture area	7067.82	58.74

SEM: Scanning electron microscopy, RB: Reciproc Blue, WOG: WaveOne Gold, OR: OneReci, RC: Plex RC-One

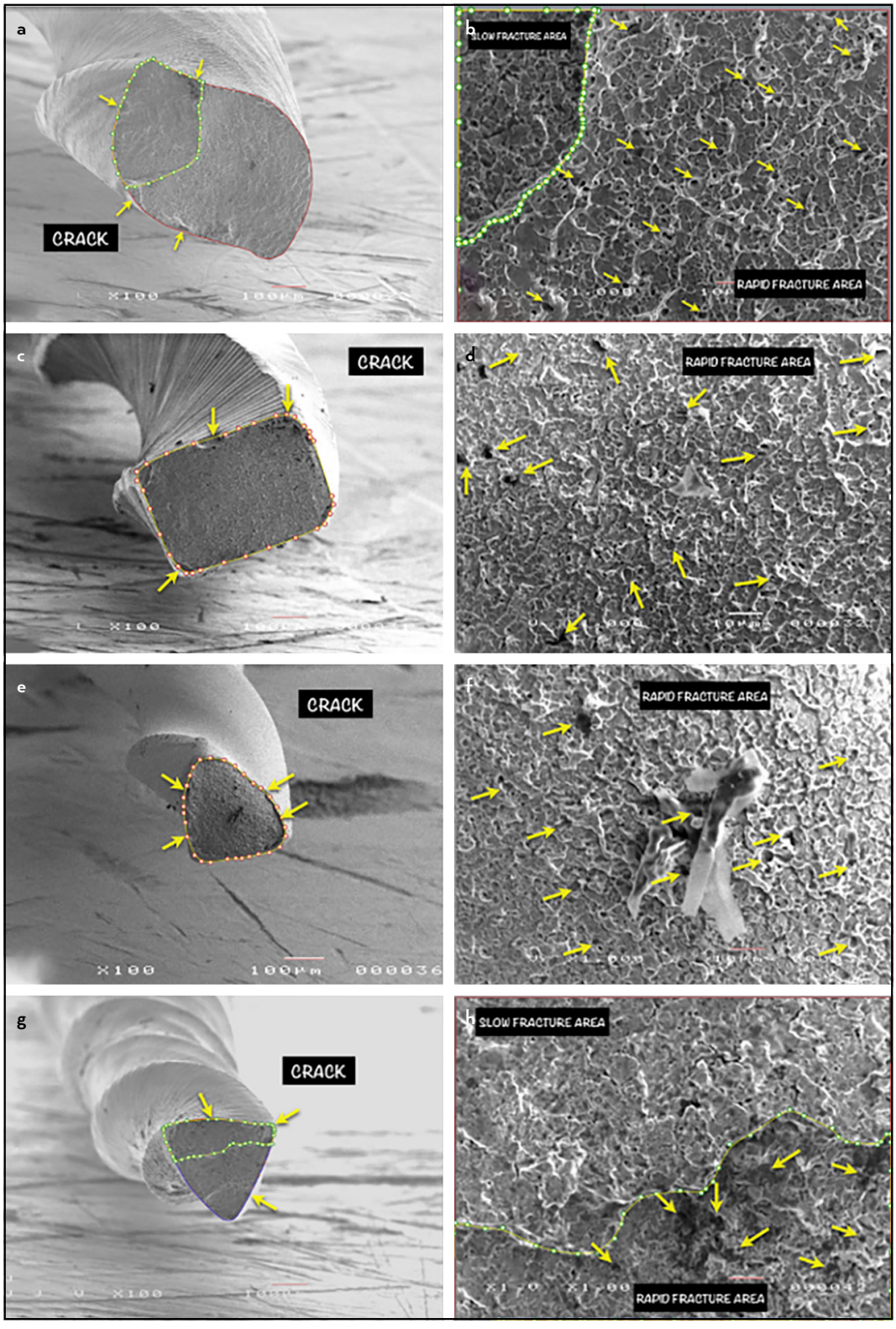

Figure 5. Fracture surface analysis of instruments under scanning electron microscopy (SEM). Reciproc Blue (RB): (a) (100X): Arrows indicate crack zones; dotted area marks the wear zone (metal deformation prior to failure). (b) (1000X): Lower section shows dimples characteristic of rapid fatigue fracture; upper section displays a small wear zone indicative of slow fracture. WaveOne Gold (WOG): (c) (100X): Arrows highlight crack zones. (d) (1000X): Arrows denote widespread dimples across the section, consistent with rapid fracture. One Reci (OR): (e) (100X): Arrows identify crack zones. (f) (1000X): Arrows point to dimples throughout the section, indicative of rapid fracture. Plex RC-One (RC-One): (g) (100X): Arrows mark crack zones; dotted area highlights the wear zone (pre-failure deformation). (h) (1000X): The lower section exhibits a small dimple area (rapid fracture due to metal fatigue); the upper section shows a large wear zone characteristic of slow fracture.

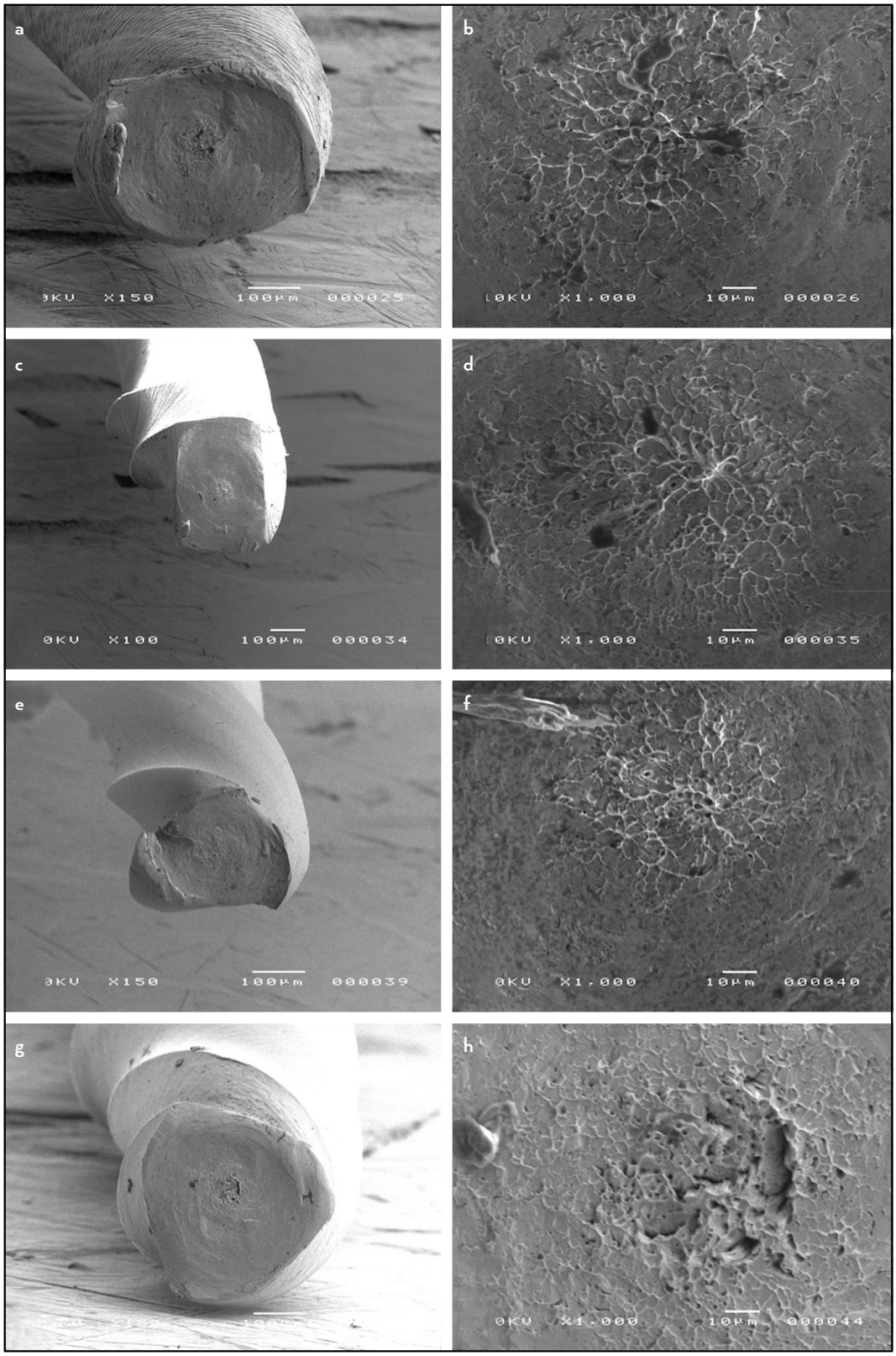

Figure 6. Torsion test results showing concentric abrasion marks and fibrous dimples at the center of rotation for all instruments, indicative of torsional failure. (a, b) Reciproc Blue (RB), (c, d) WaveOne Gold (WOG), (e, f) One Reci (OR), (g, h) Plex RC-One (RC-One)

It has been reported that artificial canals should replicate the size and taper of instruments to ensure that different nickel-titanium (NiTi) instruments can follow a consistent canal trajectory in terms of radius and curvature angle (27). However, this study faced challenges because the tested instruments had varying tapers. To standardize testing conditions, a single tapered artificial canal was utilized for all groups, featuring a diameter of 0.40 mm at the most apical portion and a taper of

0.06 mm. Although this simulated canal was not specifically designed for each instrument, all instruments fit adequately within it. Additionally, the tests were conducted at body temperature which is crucial for mimicking clinical conditions and ensuring that results apply to real clinical scenarios (28–30).

The static cyclic fatigue model was used in a laboratory-controlled environment, as described by previous studies (22, 31). In this method, the instruments are mounted in a stabilized handpiece and rotate freely in an artificial canal with predefined features and under specific conditions until the instruments fracture. This method reduces some biases, increasing the validity and reproducibility of the method, which allows a better understanding of the resistance of the behaviour of instruments. Therefore, it is questionable a recent editorial stated that the results of cyclic fatigue are useless for clinicians (32), especially under the justification that such information must be provided by the manufacturer. Additionally, an extensive discussion in the endodontic literature is moved regarding the use of a dynamic cyclic fatigue test. This methodology induces less localized mechanical stress, increasing the time and number of cycles to fatigue (33, 34). On the other hand, it is essential to emphasize that static methods can provide better information on the impact of different design features of the instruments or NiTi alloy (35).

Dynamic models also have notable disadvantages that must be considered. Depending on the design of the tube or artificial groove, torsional stress can occur, complicating the ability to distinguish the type of fatigue experienced (36). A recent critical appraisal highlighted that standardization of the axial motion of the instrument without any lateral movement inducing torsional loads is complicated. Additionally, it noted that lateral motion during the rotating instrument could induce a second bending point at the beginning of the tube or artificial groove, modifying the results of the dynamic test (32). Consequently, this study opted for static testing, as dynamic analysis may introduce additional variables beyond those related to the instrument type.

Although the artificial canal does not perfectly replicate the complexity of real root canal anatomy, the cyclic fatigue device used in this study follow the ISO specification (3630–1). Also, this artificial canal model allowed a laboratory-controlled environment and equal laboratory conditions for all instruments tested, reducing possible biases. However, it is important to emphasize that the mechanical results of the instruments can be different during root canal preparation because the clinical conditions are not the same as those of the test, which is a limitation of the method (37, 38).

The systems examined in this study—Reciproc Blue (RB), WaveOne Gold (WOG), One Reci (OR), and Plex RC-One, utilize a reciprocating motion that has been shown in the literature to enhance resistance to torsional fatigue and angular deflection relative to continuously rotating systems (12, 24). The counter-rotating cycles, characterized by low angular rotations opposite to the cutting direction, further contribute to preventing torsional fractures (28, 37). Consequently, the evaluation and comparison of these systems are highly objective, as their performance is directly linked to the specific motion employed. This allows for clinical applicability across various degrees of canal curvature complexity.

In this study, all reciprocating systems were tested under consistent conditions of speed and rotational angles, facilitating a more objective comparison. Each instrument exhibits distinct design features—such as tip geometry, transition angles, helical configurations, tapering, and cross-sectional profiles—that may account for the observed results (Table 1). These findings hold clinically relevant implications regarding the selection and application of these instruments based on their unique characteristics (39).

The systems analyzed in this study utilize martensitic alloys with varying degrees of flexibility, achieved through temperature modifications, including abrupt heating and cooling changes, as well as exposure to body temperature (33). Conducting the study at body temperature (35°±1°C) allows for results that can be directly extrapolated to clinical settings, facilitating an understanding of instrument performance across different levels of complexity. This approach highlights the impact of heat treatment on bending, torsion, and angular deflection characteristics, which are influenced by the austenite-martensite transformation and the varying austenite finishing temperatures of thermo-mechanically treated NiTi alloys (12, 18). Martensitic instruments were chosen because NiTi instruments in the austenitic phase have a superelastic tendency to straighten in curvature, pressing against the outer wall of the canal. This leads to greater resistance to displacement and an increased likelihood of fracture compared to straight canals (40). Consequently, the findings from this study are more clinically relevant than those obtained at room temperature, emphasizing the importance of instrument design and alloy properties in managing curved canals effectively.

In the flexural fatigue test, the curvature angle was standardized at 60°, combined with a radius of 5 mm, and the center of the curvature was located 5 mm from the instrument tip. Therefore, the results among the evaluated instruments can be compared, minimizing the risk of altering the outcomes (32, 41).

Fractured files were examined using SEM and intelligent automated image processing to analyze failure mechanisms. The length of fractured instruments and surface characteristics were assessed to determine if design features—such as cross-sectional profile or taper—contributed to fractures or if alloy fatigue was responsible (42).

Two types of fractures—rapid and slow—were identified using intelligent automated image processing for precise evaluation (43, 44). Rapid fractures displayed dimples under SEM analysis, indicating separation without prior deformation; conversely, slow fractures exhibited wear areas where deformation occurred before failure (45). These findings highlight how elastic and plastic deformations can precede fractures, allowing clinicians to discard instruments before catastrophic failures occur.

In the flexural fracture resistance tests, RC-One exhibited the highest resistance with a duration of 1250 seconds, significant-

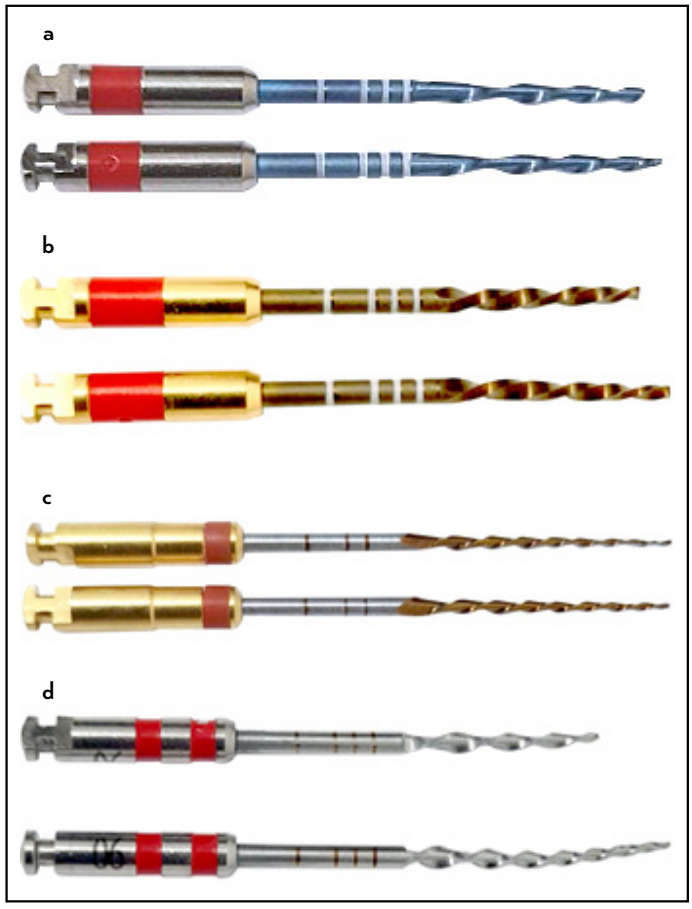

Figure 7. Locations of fracture points for each instrument: (a) Reciproc Blue (RB) fractures occurred between 3 and 5 millimeters, where the instrument's taper changes. (b) WaveOne Gold (WOG) fractures were consistently observed between 3 and 6 millimeters, corresponding to a change in the instrument's taper. (c) One Reci (OR) fractures were located between 3 and 5 millimeters, where the instrument's section profile changes. (d) Plex RC-One (RC-One) fractures occurred at various locations along the instrument, indicating metal fatigue

ly different from the other evaluated reciprocating systems. RB showed a value of 284.2 seconds, with a statistically significant difference compared to WOG, but not with OR, which showed values of 221.2 seconds. WOG exhibited the lowest cyclic fatigue resistance in bending, with a duration of 124.2 seconds.

In the case of RC-One, the fractures were observed at various locations along the instrument (Fig. 7d), indicating that the fractures resulted from continuous cyclic metal fatigue rather than an instrument design defect. The other instruments evaluated in this study may have been influenced by the 37°C temperature used during the experiments, which differs from the conditions in previous studies (37). In the case of RB, the explanation for these results may be due to its blue martensitic alloy that can be affected by the body temperature at which this study was conducted, where the alloy did not have the same resistance as RC-One (38). The fracture site in RB is between millimeter 3 and millimeter 5 (Fig. 7a) where the instrument design changes its taper. In OR, the fracture site was observed between millimeters 3 and 5 (Fig. 7c), where the cross-sectional profile changes. In WOG, the fracture site was consistently observed between 3 and 6 millimeters (Fig. 7b), where the instrument changes in taper.

These findings coincide with the observations made using SEM, where RC-One showed the largest areas of slow fracture and small areas of dimples characteristic of rapid fracture, followed by RB, which exhibited less deformation before fracture, evidenced by small areas of slow fracture (22). In contrast, both OR and WOG did not reveal wear areas characteristic of slow fracture on the fracture surface of the instrument, indicating that they do not deform before fracturing. Instead, large areas of dimples typical of rapid fracture were visible.

OR demonstrated cyclic fatigue values of 221.2 seconds, surpassing those of WOG but significantly lower than those of RC-One and RB. This disparity may be attributed to the alloy's sensitivity to the experimental conditions at body temperature. Clinically, fractures were consistently observed between 3 and 5 millimeters (Fig. 7c), where the instrument transitions from a variable triangular triple helix with a greater central mass to an S-shaped profile with a lower central mass. Despite maintaining a constant taper and variable helical angle, this design change likely impacted the instrument's fatigue resistance. Scanning electron microscopy (SEM) images (Fig. 5e, f) revealed no slow fracture wear zones on the fracture surface, indicating that the instrument did not deform before fracturing. Instead, the surface exhibited dimples characteristic of rapid fracture, which helps explain the observed results.

WOG exhibited the lowest flexural cyclic fatigue resistance, with a duration of 124.2 seconds. The temperature of 37°C during the study may have influenced its performance. Clinically, fractures were consistently noted between 3 and 6 millimeters (Fig. 7b), where the instrument transitions from 7% to 5% conicity. Its rectangular cross-section, which has a greater central mass compared to other instruments, along with a constant helical angle, likely contributed to these results. SEM images (Fig. 5c, d) also showed no wear zones indicative of slow fracture on the fracture surface, suggesting that it did not deform before fracturing. Instead, large areas of dimples characteristic of rapid fracture were evident, further elucidating the findings. Overall, the design of WOG and the properties of its alloy appeared to have a more significant impact on its performance compared to the other evaluated instruments. These findings are consistent with another study indicating that WOG performed inferiorly to RB under dynamic conditions (32).

The torsion and angular deflection tests were conducted according to ISO 3630–1, securing 3 mm of the tip and the axis of the instruments while rotating them counterclockwise at a speed of 2 RPM and a torque of 2.5 NcM at body temperature (37°C) (46). Therefore, conducting these tests under the same conditions and at body temperature makes the results more objective than if they had been performed at room temperature (47).

Regarding the torsion resistance tests, their use in reciprocating files is controversial, as the kinematics help prevent torsional fracture. In this case, the concept of angular deflection becomes particularly important (5). RB exhibited the highest torsional resistance at 1.7 Ncm, followed by RC-One at 1.32

Ncm, with no significant differences between the two. WOG ranked third with values of 1.16 Ncm, and lastly, OR showed the lowest torsional resistance values at 0.44 Ncm.

When considering the angular deflection values, the highest value corresponds to RC-One: 414.30°, followed by RB with 399.54°, OR with 390.69°, and finally WOG with 290.38 degrees. Interpreting the torsion and angular deflection values together, we find that RB and RC-One exhibited high torsional resistance with no significant differences. This similarity indicates comparable torsional resistance between the two instruments. However, RC-One demonstrated a greater angular deviation. This disparity highlights the greater plastic and elastic deformation experienced by RC-One under torsional forces before fracture. On the other hand, RC-One's greater cutting ability results in lower torsional demand for cutting compared to RB (21).

In contrast, OR and WOG exhibited lower torsion and angular deflection values, indicating a potential to reduce action time and minimize bending and torsional fatigue. OR showed the lowest torsional resistance, along with a large angle of deflection, suggesting that its alloy and design aim to control deformation by employing low torque values, which is consistent with its capacity for plastic and elastic deformation (33).

It is essential to differentiate between slow fracture and rapid fracture. Slow fracture occurs when an instrument's angular deflection leads to torsional stress, allowing it to deform without breaking. This initial deformation, known as elastic deformation, results from reversible changes in the instrument's microstructure, enabling recovery of its original shape after a temperature cycle. In contrast, permanent deformation is termed plastic deformation, which causes irreversible failures in the metallic structure and ultimately leads to fracture (48). These concepts are crucial for future studies on cyclic fracture involving advanced alloys.

Instruments that exhibit cycles or larger areas of slow fracture demonstrate greater angular deflection, allowing for plastic deformations before fracture. This characteristic enhances their resistance to flexural and torsional stress (49), a finding supported by the results of this study.

In the bending test, RC-One exhibited the greatest flexibility among all the instruments, maintaining its shape as a characteristic of controlled memory, followed by RB, which demonstrated much lower flexibility and controlled memory. OR and WOG did not show a good degree of flexibility. This property is essential for withstanding the results of cyclic flexural fatigue, and its clinical applicability is important for preserving controlled memory (22). Such flexibility is particularly beneficial in managing curved canals.

Taking all the results of the study into account, finding clinical applicability is of utmost importance for the endodontist. With knowledge of the alloys and designs of the instruments, it can be inferred that RC-One is the safest instrument for any type of curvature, especially in severe curves. RB is an option for clinicians to manage curvatures, while OR and WOG are suitable for managing moderate curvatures. Thus, with the limitations of this study, it was found that RC-One presents significantly higher levels of cyclic fatigue resistance in simulated canals with severe curvatures compared to RB, OR, and WOG, respectively. The torque resistance values are very similar for RB and RC-One, being significantly higher than those of OR and WOG. Additionally, the degree of angular deflection showed that RC-One yielded better results than RB, OR, and WOG.

One of the limitations of this study is that the use of artificial canals does not fully replicate the complexity of natural root canal anatomy. While artificial models allow for controlled experimentation, they may not accurately reflect the intricate anatomical variations and irregularities found in real teeth. This discrepancy could impact the generalizability of the findings to clinical scenarios, as the behavior of endodontic instruments in artificial canals may differ from their performance in actual root canal systems. Future recommendations include conducting similar studies with larger sample sizes that incorporate diverse root canal anatomies or test additional instrument systems.

CONCLUSION

Based on the limitations of this study, it was observed that the best performance in the bending test was obtained by Plex RC-One, followed by Reciproc Blue, while the most failures were observed in WaveOne Gold and One Reci. Plex RC-One exhibits significantly higher levels of resistance to cyclic fatigue in simulated canals with severe curvatures compared to Reciproc Blue, WaveOne Gold, and One Reci. Regarding torque resistance, Reciproc Blue and Plex RC-One demonstrate similar levels, surpassing One Reci and WaveOne Gold. Additionally, Plex RC-One displayed superior results in angular deflection compared to Reciproc Blue, One Reci, and WaveOne Gold. Therefore, it can be inferred that Plex RC-One is an excellent choice for managing canals with severe curvatures, while Reciproc Blue, WaveOne Gold, and One Reci are suitable options for handling mild to moderate curvatures.

Disclosures

Ethics Committee Approval: The study was approved by the Santa Maria University Ethics Committee (no: CBUSM-0723, date: 03/15/2023).

Authorship Contributions: Concept – J.C.B., R.P.; Design – J.C.B.; Supervision – J.C.B.; Funding – J.C.B.; Materials – J.C.B.; Data collection and/or processing – A.T.C., M.P.A., M.A.H.D.; Data analysis and/or interpretation – H.R.M.; Literature search – H.D.M.A., J.O.F.; Writing – M.M.G., J.F.G.S.; Critical review – J.F.G.S.

Conflict of Interest: All authors declared no conflict of interest.

Use of AI for Writing Assistance: The authors declared that the study used mainly two software Image J and Rhinoceros 8.0 with the aid of Learning Machine IA as stated in the Methods section in the Descriptive area Analysis section.

Financial Disclosure: The authors declared that this study received no financial support.

Peer-review: Externally peer-reviewed.

REFERENCES

1. Caballero-Flores H, Nabeshima CK, Binotto E, Machado MEL. Fracture incidence of instruments from a single-file reciprocating system by students in an endodontic graduate programme: a cross-sectional retrospective study. Int Endod J 2019; 52(1):13–8. [CrossRef]
2. Iqbal MK, Kohli MR, Kim JS. A retrospective clinical study of incidence of root canal instrument separation in an endodontics graduate program: a PennEndo database study. J Endod 2006; 32(11):1048–52. [CrossRef]

3. Madarati AA, Watts DC, Qualtrough AJE. Opinions and attitudes of endodontists and general dental practitioners in the UK towards the intra-canal fracture of endodontic instruments. Part 2. Int Endod J 2008; 41(12):1079–87. [CrossRef]
4. Gambarini G, Galli M, Seracchiani M, Di Nardo D, Versiani MA, Piasecki L, et al. *In vivo* evaluation of operative torque generated by two nickel-titanium rotary instruments during root canal preparation. Eur J Dent 2019; 13(4):556–62. [CrossRef]
5. Gambarini G, Testarelli L, Milana V, Pecci R, Bedini R, Pongione G, et al. Angular deflection of rotary nickel titanium files: a comparative study. Ann Ist Super Sanita 2009; 45(4):423–6. [CrossRef]
6. Sattapan B, Nervo GJ, Palamara JE, Messer HH. Defects in rotary nickel-titanium files after clinical use. J Endod 2000; 26(3):161–5. [CrossRef]
7. Zubizarreta-Macho Á, Alonso-Ezpeleta Ó, Martínez AA, Matoses VF, Brucheli JC, Agustín-Panadero R, et al. Novel electronic device to quantify the cyclic fatigue resistance of endodontic reciprocating files after using and sterilization. Appl Sci 2020; 10(14):4962. [CrossRef]
8. Ríos-Osorio N, Caviedes-Bucheli J, Murcia-Celedón J, Gutiérrez C, Sierra-Collazo D, Alvarado-Caicedo B, et al. Comparison of dynamic cyclic fatigue resistance of Reciproc® Blue and WaveOne® Gold after sterilization and/or immersion in sodium hypochlorite. J Clin Exp Dent 2024; 16(1):e1–10. [CrossRef]
9. Uslu G, Gundogar M, Özyurek T, Plotino G. Cyclic fatigue resistance of reduced-taper nickel-titanium (NiTi) instruments in doubled-curved (S-shaped) canals at body temperature. J Dent Res Dent Clin Dent Prospects 2020; 14(2):111. [CrossRef]
10. Hou XM, Yang YJ, Qian J. Phase transformation behaviors and mechanical properties of NiTi endodontic files after gold heat treatment and blue heat treatment. J Oral Sci 2020; 63(1):8–13. [CrossRef]
11. Nehme W, Naaman A, Diemer F, Leotta ML, La Rosa GRM, Pedullà E. Influence of different heat treatments and temperatures on the cyclic fatigue resistance of endodontic instruments with the same design. Clin Oral Investig 2023; 27(4):1793–8. [CrossRef]
12. Schäfer E, Bürklein S, Donnermeyer D. A critical analysis of research methods and experimental models to study the physical properties of NiTi instruments and their fracture characteristics. Int Endod J 2022; 55(S1):72–94. [CrossRef]
13. Chaniotis A, Ordinola-Zapata R. Present status and future directions: management of curved and calcified root canals. Int Endod J 2022; 55(S3):656–84. [CrossRef]
14. Setzer FC, Böhme CP. Influence of combined cyclic fatigue and torsional stress on the fracture point of nickel-titanium rotary instruments. J Endod 2013; 39(1):133–7. [CrossRef]
15. Terauchi Y, Ali WT, Abielhassan MM. Present status and future directions: removal of fractured instruments. Int Endod J 2022; 55(S3):685–709. [CrossRef]
16. De-Deus G, Canabarro A. Strength of recommendation for single-visit root canal treatment: grading the body of the evidence using a patient-centred approach. Int Endod J 2017; 50(3):251–9. [CrossRef]
17. Keskin C, Inan U, Demiral M. Effect of interrupted motion on the cyclic fatigue resistance of reciprocating nickel-titanium instruments. Int Endod J 2018; 51(5):549–55. [CrossRef]
18. Yamakami SA, Gallas JA, Petean IBF, Souza-Gabriel AE, Sousa-Neto M, Macedo AP, et al. Impact of endodontic kinematics on stress distribution during root canal treatment: analysis of photoelastic stress. J Endod 2022; 48(2):255–62. [CrossRef]
19. MicroMega. MicroMega One RECI, unique reciprocating file for exploring opposite directions. Available at: https://micro-mega.com/shaping/one-reci/?lang=en. Accessed Apr 4, 2024.
20. Moriya PT, de Carvalho KKT, Kishen A, Souza EM, Versiani MA. Quasi-3D dynamic photoelastic analysis of stress distribution during preparation of simulated canals with 13 mechanical preparation systems. Int Endod J 2023; 56(11):1399–411. [CrossRef]
21. Orodeka. PLEX RC-ONE. Available at: https://www.orodeka.com/plex-rc-one/. Accessed Aug 4, 2024.
22. Alcalde MP, Duarte MAH, Bramante CM, de Vasconselos BC, Tanomaru-Filho M, Guerreiro-Tanomaru JM et al. Cyclic fatigue and torsional strength of three different thermally treated reciprocating nickel-titanium instruments. Clin Oral Investig 2018; 22(4):1865–71. [CrossRef]
23. Bahia MGA, Melo MCC, Buono VTL. Influence of simulated clinical use on the torsional behavior of nickel-titanium rotary endodontic instruments. Oral Surg Oral Med Oral Pathol Oral Radiol Endod 2006; 101(5):675–80. [CrossRef]
24. Caviedes-Bucheli J, Rios-Osorio N, Usme D, Jimenez C, Pinzon A, Rincón Jyahata, et al. Three-dimensional analysis of the root canal preparation with Reciproc Blue®, WaveOne Gold® and XP EndoShaper®: a new method *in vivo*. BMC Oral Health 2021; 21(1):88. [CrossRef]
25. Rhino3D. Rhino3D Education. Available at: https://www.rhino3d.education/. Accessed Aug 4, 2024.
26. Faggion CM. Guidelines for reporting pre-clinical *in vitro* studies on dental materials. J Evidence-Based Dent Prac 2012; 12(4):182–9. [CrossRef]
27. Plotino G, Grande NM, Cordaro M, Testarelli L, Gambarini G. A review of cyclic fatigue testing of nickel-titanium rotary instruments. J Endod 2009; 35(11):1469–76. [CrossRef]
28. Gavini G, Santos MD, Caldeira CL, Machado MEL, Freire LG, Iglecias EF, et al. Nickel-titanium instruments in endodontics:a concise review of the state of the art. Braz Oral Res 2018; 32(Suppl 1):e67. [CrossRef]
29. Jamleh A, Alghaihab A, Alfadley A, Alfawaz H, Alqedairi A, Alfouzan K. Cyclic fatigue and torsional failure of EdgeTaper Platinum endodontic files at simulated body temperature. J Endod 2019; 45(5):611–4. [CrossRef]
30. Klymus ME, Alcalde MP, Vivan RR, Só MVR, de Vasconselos BC, Duarte MAH. Effect of temperature on the cyclic fatigue resistance of thermally treated reciprocating instruments. Clin Oral Investig 2019; 23(7):3047–52. [CrossRef]
31. Alcalde MP, Tanomaru-Filho M, Bramante CM, Duarte MAH, Guerreiro-Tanomaru JM, Camilo-Pinto J, et al. Cyclic and torsional fatigue resistance of reciprocating single files manufactured by different nickel-titanium alloys. J Endod 2017; 43(7):1186–91. [CrossRef]
32. Hülsmann M. Research that matters: studies on fatigue of rotary and reciprocating NiTi root canal instruments. Int Endod J 2019; 52(10):1401–2. [CrossRef]
33. Pedullà E, Lizio A, Scibilia M, Grande NM, Plotino G, Boninelli S, et al. Cyclic fatigue resistance of two nickel-titanium rotary instruments in interrupted rotation. Int Endod J 2017; 50(2):194–201. [CrossRef]
34. De-Deus G, Leal Vieira VT, Nogueira da Silva EJ, Lopes H, Elias CN, Moreira EJ. Bending resistance and dynamic and static cyclic fatigue life of Reciproc and WaveOne large instruments. J Endod 2014; 40(4):575–9. [CrossRef]
35. Saber S, Fawzy AS. Effect of thermal treatment on the flexural resistance of mechanically pre-fatigued NiTi rotary endodontic files. ENDO 2011; 5(2):145–50.
36. Dederich DN, Zakariasen KL. The effects of cyclical axial motion on rotary endodontic instrument fatigue. Oral Surg Oral Med Oral Pathol 1986; 61(2):192–6. [CrossRef]
37. Odgerel Z, Kwak SW, Ha JH, Gambarini G, Shen Y, Kim HC. Effect of MT technology of heat treatment on Reciproc: comparison of Reciproc, Reciproc Blue, and Reciproc MT. J Endod 2024; 50(4):520–6. [CrossRef]
38. Plotino G, Grande NM, Testarelli L, Gambarini G, Castagnola R, Rossetti A, et al. Cyclic fatigue of Reciproc and Reciproc Blue Nickel-titanium reciprocating files at different environmental temperatures. J Endod 2018; 44(10):1549–52. [CrossRef]
39. De-Deus G, Cardoso ML, Simões-Carvalho M, Silva EJNL, Belladonna FG, Cavalcante DM, et al. Glide path with reciprocating driven pathfinding instrument: performance and fracture rate. J Endod 2021; 47(1):100–4. [CrossRef]
40. Özyürek T, Yılmaz K, Uslu G. Shaping ability of Reciproc, WaveOne GOLD, and HyFlex EDM single-file systems in simulated S-shaped canals. J Endod 2017; 43(5):805–9. [CrossRef]
41. Sobotkiewicz T, Huang X, Haapasalo M, Mobuchon C, Hieawy A, Hu J, et al. Effect of canal curvature location on the cyclic fatigue resistance of reciprocating files. Clin Oral Investig 2021; 25(1):169–77. [CrossRef]
42. Zhang EW, Cheung GSP, Zheng YF. Influence of cross-sectional design and dimension on mechanical behavior of nickel-titanium instruments under torsion and bending: a numerical analysis. J Endod 2010; 36(8):1394–8. [CrossRef]
43. Mohammad-Rahimi H, Sohrabniya F, Ourang SAH, Dianat O, Aminoshariae A, Nagendrababu V, et al. Artificial intelligence in endodontics: Data preparation, clinical applications, ethical considerations, limitations, and future directions. Int Endod J 2024; 57(11):1566–95. [CrossRef]

44. Chen J, Balan A, Masih Das P, Thiruraman JP, Drndić M. Computer vision AC-STEM automated image analysis for 2D nanopore applications. Ultramicroscopy 2021; 231:113249. [CrossRef]
45. Ertuğrul İF, Arslan HK. Investigation of four nickel titanium endodontic instruments, with cyclic fatigue resistance, scanning electron microscopy, and energy dispersive x-ray spectroscopy. Microsc Res Tech 2024; 87(11):2801–7. [CrossRef]
46. Yahata Y, Yoneyama T, Hayashi Y, Ebihara A, Doi H, Hanawa et al. Effect of heat treatment on transformation temperatures and bending properties of nickel-titanium endodontic instruments. Int Endod J 2009; 42(7):621–6. [CrossRef]
47. Drukteinis S, Peciuliene V, Dummer PMH, Hupp J. Shaping ability of BioRace, ProTaper NEXT and Genius nickel-titanium instruments in curved canals of mandibular molars: a MicroCT study. Int Endod J 2019; 52(1):86–93. [CrossRef]
48. Suter B, Lussi A, Sequeira P. Probability of removing fractured instruments from root canals. Int Endod J 2005; 38(2):112–23. [CrossRef]
49. Kim HC, Kwak SW, Cheung GSP, Ko DH, Chung SM, Lee W. Cyclic fatigue and torsional resistance of two new nickel-titanium instruments used in reciprocation motion: Reciproc versus WaveOne. J Endod 2012; 38(4):541–4. [CrossRef]